

# X-ray Spectroscopy of the Nearby, Classical T Tauri Star TW Hya

Joel H. Kastner<sup>1</sup>, David P. Huenemoerder, Norbert S. Schulz

Center for Space Research, Massachusetts Institute of Technology, NE80-6007, Cambridge, MA  
02139

e-mail: jhk@juggler.mit.edu

and

David A. Weintraub

Department of Physics & Astronomy, Vanderbilt University, P.O. Box 1807 Station B, Nashville,  
TN 37235

*To appear in the The Astrophysical Journal  
(Received 1999 April 28; accepted 1999 May 24)*

## ABSTRACT

We present *ASCA* and *ROSAT* X-ray observations of the classical T Tauri star TW Hya, the namesake of a small association that, at a distance of  $\sim 50$  pc, represents the nearest known region of recent star formation. Analysis of *ASCA* and *ROSAT* spectra indicates characteristic temperatures of  $\sim 1.7$  MK and  $\sim 9.7$  MK for the X-ray emitting region(s) of TW Hya, with emission lines of highly ionized Fe dominating the spectrum at energies  $\sim 1$  keV. The X-ray data show variations in X-ray flux on  $\lesssim 1$  hr timescales as well as indications of changes in X-ray absorbing column on timescales of several years, suggesting that flares and variable obscuration are responsible for the large amplitude optical variability of TW Hya on short and long timescales, respectively. Comparison with model calculations suggests that TW Hya produces sufficient hard X-ray flux to produce significant ionization of molecular gas within its circumstellar disk; such X-ray ionization may regulate both protoplanetary accretion and protoplanetary chemistry.

*Subject headings:* X-rays: stars — stars: pre-main-sequence: individual (TW Hya) — stars: variable — stars: circumstellar matter

---

<sup>1</sup>Address as of 7/15/99: Rochester Institute of Technology, Chester F. Carlson Center for Imaging Science, 84 Lomb Memorial Drive, Rochester, NY 14623

## 1. Introduction

A primary result of X-ray surveys of star formation regions by the *Einstein* and *ROSAT* X-ray satellite observatories is the association of strong X-ray emission with solar-mass, pre-main sequence (PMS) stars at various stages of evolution (e.g., Montmerle et al. 1993; Feigelson 1996; and references therein). This result, when viewed in the context of recent theoretical predictions concerning the potentially profound effects of X-rays from young stars on the physics and chemistry of their circumstellar, protoplanetary disks (e.g., Glassgold, Najita, & Igea 1997; Igea & Glassgold 1999), makes clear that knowledge of the detailed X-ray spectra of pre-main sequence stars is central to an understanding of the early evolution of the Sun and solar system. Low-mass PMS stars in Taurus-Auriga, Chamaeleon, Lupus, and Ophiuchus are intrinsically 2–4 orders of magnitude more X-ray luminous than the Sun; however, as a result of the large ( $\sim 150$  pc) distances to these “local” regions of active star formation and, in many cases, the large X-ray absorbing column depths characteristic of the dark clouds in which the PMS stars reside, these stars’ X-ray fluxes rarely exceed  $10^{-12}$  ergs/cm<sup>2</sup>/s except during strong flares. Thus, it is difficult to perform X-ray spectroscopy of individual pre-main sequence stars that are located in well-studied regions of star formation.

As a consequence of these limitations, the X-ray emission mechanisms of PMS stars remain poorly understood. However, the available evidence suggests that coronal activity is the source of X-rays from low-mass PMS stars. Until quite recently, most of the evidence was indirect and based on, e.g., the observed continuum of X-ray activities from pre-main sequence through early main sequence evolution and the generally large rotation rates and X-ray-flaring behavior of T Tauri stars (Kastner et al. 1997 [hereafter KZWF]; Skinner et al. 1997; and references therein). These observations support a scaled-up solar dynamo model underlying the X-ray emission from low-mass PMS stars (e.g., Carkner et al. 1996). With the advent of the *ASCA* X-ray satellite observatory, direct spectroscopic evidence also is accumulating in support of a coronal origin for the X-rays (e.g., Carkner et al.; Skinner et al.; Skinner & Walter 1998). Generally, *ASCA* spectra of PMS stars obtained to date can be well modeled as arising in coronal plasma with a bimodal temperature distribution characterized by temperatures of  $\sim 3 - 30$  MK. Thus, *ASCA* observations have provided new impetus to the study of PMS stellar X-ray sources.

To better understand what role X-ray emission may play in the chemical and physical evolution of circumstellar material, and thereby test the predictions of recent theory (Glassgold, Najita, & Igea 1997; Shu et al. 1997), we must obtain high-quality X-ray spectra of individual PMS stars that are directly analogous to the primordial Sun and solar system. Such data can also provide probes of intervening circumstellar material, via the spectral

signature of absorption of soft X-rays. With a few exceptions (e.g., Skinner & Walter 1998), however, *ASCA* investigations have focused either on deeply embedded protostars whose nature and evolutionary status is uncertain, or on highly active, weak-lined TTS. Classical TTS — i.e., TTS surrounded by massive disks that are the likely sites of planet formation — have largely been neglected by *ASCA* studies of PMS stars, mostly due to the difficulty in identifying suitably X-ray bright candidates.

The classical TTS TW Hya, noteworthy for its large projected distance from the nearest dark cloud (Rucinski & Krautter 1983), is a particularly interesting object in this regard. KZWF established that TW Hya belongs to a small group of T Tauri star (TTS) systems likely comprising a physical association (the TW Hya Association; hereafter TWA). These TTS systems form an exceptionally bright group in X-rays compared with TTS in Taurus and Chamaeleon, suggesting they are quite close to the Earth. Indeed, on the basis of *ROSAT* X-ray and other data, KZWF concluded that the TWA stars are 10–30 Myr old and thus, based on theoretical PMS evolutionary tracks, the Association lies a mere  $\sim 50$  pc distant. Hipparcos distances to Association members TW Hya and HD 98800 — 57 pc (Wichmann et al. 1998) and 48 pc (Soderblom et al. 1998), respectively — confirm these results, although there is growing evidence that the ages of most of the Association stars lie in the range 5 to 15 Myr (Webb et al. 1998; Weintraub et al. 1999). Hence the TW Hya Association, consisting of a small population of T Tauri stars with no known associated cloud, probably represents the nearest region of recent star formation. Recently, Webb et al. identified another five PMS/TTS systems that are likely members of the TWA.

Though all of the late-type TWA members display various TTS characteristics, such as  $H\alpha$  emission, Li absorption, and/or IR excesses, TW Hya is the only TWA star to display both strong  $H\alpha$  (Rucinski & Krautter 1983) and submillimeter continuum emission (Weintraub, Sandell, & Duncan 1989). It is also the only known CO emission line source among the TWA stars (Zuckerman et al. 1995) and, furthermore, displays submillimeter emission lines of  $^{13}\text{CO}$ , HCN, CN, and  $\text{HCO}^+$  (KZWF), despite the apparent lack of interstellar molecular gas in its vicinity. KZWF conclude that, given the narrow ( $\sim 0.7$  km  $\text{s}^{-1}$ ) observed molecular emission line widths, TW Hya possesses a dusty molecular disk that is viewed nearly face-on. Considering the  $\sim 20$  Myr age of TW Hya, this disk may closely resemble the solar nebula at a time during, or shortly after, the formation of Jupiter.

Among the small but growing number of PMS solar analogs known to possess circumstellar, molecular disks, TW Hya is the brightest in X-rays. Furthermore, it is found in relative isolation, with no nearby X-ray sources or intervening dark cloud material, and we likely view its star-disk system nearly pole-on (KZWF). For these reasons, TW Hya presents an excellent subject for X-ray spectroscopy with *ASCA*, which features X-ray

spectral resolution and spectral coverage superior to that of *ROSAT* but spatial resolution inferior to that of its immediate predecessor. In this paper, we present and analyze *ASCA* data we acquired for TW Hya and also re-analyze archival *ROSAT* pointed observations (Hoff et al. 1998). The results of this analysis provide constraints for models of X-ray irradiation of circumstellar molecular gas and, more generally, serve as a starting point for inferences concerning the primordial solar X-ray spectrum at the epoch of Jovian planet formation. The results also shed light on the well-documented but puzzling optical variability of TW Hya.

## 2. Observations

### 2.1. ASCA

TW Hya was observed with the two Solid-state Imaging Spectrometers (SIS) and two Gas Imaging Spectrometers (GIS) aboard *ASCA* on 1997 June 26-27. Both types of detectors are sensitive from  $\sim 0.5$  keV to  $\sim 10$  keV. The two SIS instruments afford superior broad-band sensitivity and spectral resolution ( $E/\Delta E \sim 30$  at 6.7 keV), while the two GIS are somewhat more sensitive than the SIS at higher energies. For these observations, 2 of the 4 available CCDs in each SIS detector were active. This configuration allowed us sufficient off-source detector field of view to determine background count rates and spectra, while limiting the reporting of spurious events from off-source CCDs.

Data reduction was accomplished via standard processing software provided by the High Energy Astrophysics Science Archive Research Center (HEASARC). We used standard screening criteria (via the HEASARC XSELECT software) to screen event data on the basis of Earth elevation angles, particle background levels, and event CCD pixel distributions, and to reject hot and flickering CCD pixels, thereby producing lists of valid X-ray events. To maximize signal to noise ratio, we have combined data telemetered at “medium” and “low” bit rates with data telemetered at “high” bit rate. The resulting SIS dataset may, in principle, exhibit slightly degraded spectral resolution relative to a dataset constructed from the “high” bit rate data alone, since data obtained in “medium” and “low” bit rates cannot be corrected for the so-called “echo effect” in the SIS CCDs. We cannot discern any such degradation in the combined dataset relative to that of the “high” bit rate data alone, however, and hence the inclusion of “medium” and “low” bit rate data improves the analysis presented below. Resulting net (post-screening) exposure times were 31.1 ks for each SIS detector and 31.4 ks for each GIS detector, out of the total observation duration of  $\sim 94$  ks ( $\sim 1.1$  days).

Within the  $\sim 40'$  diameter GIS and  $\sim 11' \times 22'$  SIS fields, TW Hya is the only X-ray source detected. We extracted events in  $4'$  (SIS) and  $6'$  (GIS) radii circles centered on the position of the source, to determine count rates and to accumulate spectra (§3.2.1). We also extracted events in off-source regions of each detector, again using extraction radii of  $4'$  (SIS) and  $6'$  (GIS), to obtain representative background count rates and spectra. These background regions were located  $\sim 12'$  away from the source regions and hence are very unlikely to be contaminated with source photons, given the modest count rates of TW Hya. Results for count rates are listed in Table 1.

## 2.2. ROSAT

TW Hya was the target of a pointed *ROSAT* Position Sensitive Proportional Counter (PSPC) observation on 1991 December 12, and is also included in the *ROSAT* All-Sky Survey (RASS) Bright Source Catalog (Voges et al. 1998). Here we re-analyze the pointed PSPC data, which were summarized in KZWF and subsequently presented in more detail by Hoff et al. (1998). The X-ray sensitivity of the PSPC plus *ROSAT* X-ray telescope extends from about 0.1 keV to 2.4 keV, with energy resolution of  $\sim 40\%$  at  $\sim 1$  keV. We find that a total of 2100 counts were obtained for TW Hya in 6.8 ks of detector live time. This count rate,  $309 \pm 7$  counts  $\text{ks}^{-1}$ , is consistent with the count rate listed in Table 2 of Hoff et al. The background count rate, as estimated from off-source regions of the PSPC image, was  $< 6$  counts  $\text{ks}^{-1}$ .

## 3. Results

### 3.1. ROSAT

The PSPC spectrum, binned into 34 energy channels, is displayed in Fig. 2 (see also Fig. 2 of Hoff et al. 1998). The spectrum is double-peaked, with peaks near 0.25 and 0.9 keV, and is similar to PSPC spectra of certain Taurus-Auriga T Tauri stars that are located along lines of sight with relatively little intervening cloud material (Carkner et al. 1996). Our tests of fits of pure continuum emission models, such as blackbody or thermal bremsstrahlung emission, indicate that such models cannot match the observed shape of the PSPC spectrum peak near 0.9 keV. Pure continuum models are also ruled out, somewhat more emphatically, by the *ASCA* data (§3.2.1). Thus, to fit the PSPC spectrum, we adopt the popular model for X-ray emission from active stars, i.e., Raymond-Smith (R-S) coronal plasma emission suffering intervening absorption due to circumstellar and/or interstellar

gas. The R-S models assume collisional ionization equilibrium, and include both emission lines and continuum contributions for a given temperature and set of elemental abundances (Raymond & Smith 1976). We attempted fits of both single-component and two-component R-S models, with solar abundances. After convolving with the ROSAT/PSPC spectral response, we find that the latter model, consisting of a linear combination of R-S models at two different temperatures, provides a superior fit to the PSPC data. Results for the best-fit R-S model parameters are listed in Table 2, and the model (folded through the PSPC spectral response) is overlaid on the data in Fig. 1. The best-fit characteristic temperatures of  $kT_1 = 0.14$  keV ( $T_1 = 1.7$  MK) and  $kT_2 = 0.85$  keV ( $T_2 = 9.7$  MK) for the soft and hard emission components, respectively, are similar to results obtained by Hoff et al. (1998).

A light curve extracted from the pointed PSPC data (not shown) indicates that, in contrast to the *ASCA* observations (§3.2.2), the X-ray flux from TW Hya was nearly constant during the *ROSAT* observing intervals. However, the RASS count rate ( $570 \pm 40$  counts  $\text{ks}^{-1}$ ; KZWF) is approximately double that of the pointed observations. Our event extraction radius for the pointed data is sufficiently large to rule out differences in extraction radii as the origin of the different RASS and pointed count rates. Thus it appears that, like typical TTS, TW Hya probably is variable in X-rays.

## 3.2. ASCA

### 3.2.1. Spectral analysis

We extracted source spectra from the screened SIS0 and SIS1 event lists using uniform bins of width 29 eV for both instruments. Although the count rates of the two instruments differ by  $\sim 30\%$  due to different detector sensitivities (Table 1), the resulting SIS0 and SIS1 spectra appear very similar. In particular, source spectra obtained with both instruments peak at about 0.95 keV and display plateaus or “shoulders” of emission on either side of this peak; these shoulders are centered at about 0.75 keV and 1.3 keV. Other features are also well reproduced in the corresponding source and background spectra, and tests of independent fits to the SIS0 and SIS1 source spectra yield similar results for the two datasets for model parameters such as emitting region temperature and intervening absorbing column (see below), suggesting the SIS0 and SIS1 data can be combined without compromising spectral response. Hence, to maximize signal-to-noise, we averaged the SIS0 and SIS1 source spectra, and then subtracted the average of the SIS0 and SIS1 background spectra from the resulting source spectrum. A weak high-energy tail that is present in the “raw” source spectra is also present in the background spectra, suggesting it is not intrinsic to the source; this feature largely disappears from the combined SIS spectrum of TW Hya

once background is subtracted (Fig. 2). We performed all subsequent spectral analysis on this combined, background-subtracted SIS0 and SIS1 spectrum (which we hereafter refer to as the TW Hya SIS spectrum), using a hybrid spectral response matrix constructed from a weighted average of the SIS0 and SIS1 response matrices for the appropriate regions of the detectors.

Attempts to fit pure continuum models, such as blackbody emission and thermal bremsstrahlung emission, fail to reproduce the relatively sharp peak in the spectrum near 0.95 keV. Significantly improved fits are obtained once line emission is included. In particular, R-S thermal plasma models with characteristic temperatures  $\sim 10$  MK (and solar metallicities) reproduce the intensity and overall shape of the observed 0.95 keV peak (Fig. 2). We therefore conclude that this feature is dominated by a complex of lines generated by highly ionized species of Fe, as these lines dominate the spectra of  $\sim 10$  MK R-S models in the spectral region near  $\sim 1$  keV.

We find that single-component R-S models are not able to simultaneously fit the 0.95 keV peak and the low-energy ( $< 0.7$  keV) tail in the SIS spectrum. This residual tail of emission suggests the presence of an additional, softer component. As the presence of a soft component is also required to fit the PSPC spectrum of TW Hya (§3.1; Hoff et al. 1998), we attempted fits with two-component R-S models. We did not attempt to use the PSPC spectral fitting results to constrain the temperatures of the R-S model fits to the *ASCA* data, in light of the  $\sim 5.5$  year time interval between the *ROSAT* and *ASCA* observations. Over this interval there is the possibility of variations in the physical conditions of the X-ray emitting region(s) and/or in the distribution of absorbing material along the line of sight to the star. If we use the results of PSPC spectral analysis to constrain the absorbing column toward TW Hya at  $N_H = 5 \times 10^{20} \text{ cm}^{-2}$ , we find characteristic temperatures of  $\sim 2.4$  MK and  $\sim 12$  MK, respectively, for the soft and hard components in the *ASCA* spectrum (Table 2; Fig. 2). If, on the other hand, we allow  $N_H$  to be a free parameter, we find from the SIS spectrum characteristic temperatures that are very similar to those obtained from our independent fit to the PSPC data, albeit with substantially larger emission measures for both soft and hard components (since the best-fit  $N_H$  is larger than that obtained from the fit to the PSPC spectrum). The fit with  $N_H$  unconstrained also represents a marginal improvement over that obtained by holding  $N_H$  fixed at  $5 \times 10^{20} \text{ cm}^{-2}$ , particularly in the  $\sim 1$  keV spectral region. The results of the *ASCA*/SIS fit with  $N_H$  unconstrained would suggest that  $N_H$  was larger by a factor of  $\sim 6$  at the epoch of the *ASCA* observations.

We followed a similar procedure to perform spectral analysis of GIS data. Source spectra were extracted from the screened GIS2 and GIS3 event lists using uniform bins of width 47 eV. These spectra were combined, and the combined background spectrum was

subtracted from this combined source spectrum to produce the final GIS spectrum (Figure 3). This spectrum, like the SIS spectrum, displays a sharp peak at  $\sim 1$  keV. A hybrid instrument response matrix was constructed for purposes of spectral fitting. Fits to the GIS spectrum were constrained by the results of PSPC and SIS model fitting. Specifically, we used these results to obtain two separate fits to the GIS spectrum, with  $N_H$  fixed at  $5 \times 10^{20} \text{ cm}^{-2}$  and emission temperature fixed at  $kT = 0.98$  keV, and with  $N_H$  fixed at  $2.9 \times 10^{21} \text{ cm}^{-2}$  and emission temperature fixed at  $kT = 0.86$  keV. We did not include a soft component corresponding to those used in the PSPC and SIS model fitting, in light of the poor soft X-ray response of the GIS detectors. With these constraints, we obtain good fits to the GIS spectrum (Table 2; Fig. 2) at energies  $< 2$  keV, provided we apply an offset of 0.1 keV in the energy scale of the GIS response function. These fits suggest the presence of an additional, harder emission component in the GIS spectrum (Fig. 2), although due to the small count rates at channel energies  $> 2$  keV we are unable to determine a unique emission temperature for this potential, additional component.

### 3.2.2. Temporal Analysis

A light curve extracted from the SIS and GIS event lists is presented in Fig. 2. The merged GIS and SIS light curve shows some evidence for sudden, short-lived increases in X-ray flux. These “flares” (detected  $\sim 0.15$  and  $\sim 0.87$  days after the start of the observation) were of duration  $\sim 1$  hour, separated by about 0.72 days, and represented a doubling to tripling of the count rate. The increases were observed independently in all four detectors; therefore, we are able to rule out background or instrumental effects as the source of these count rate fluctuations. Spectra extracted from time intervals at high count rate yield fit results for model parameters that are the same to within the uncertainties as those obtained for spectra extracted from the entire observation interval. Hence it appears there were no significant changes in the X-ray spectrum of TW Hya during the periods of increased X-ray flux, although the relatively low signal-to-noise ratios of *ASCA* spectra obtained during these periods preclude a definitive comparison.

The apparent modest flaring detected in the *ASCA* observations of TW Hya stands in contrast to the strong, long-lived flares that have been detected during *ASCA* observations of deeply embedded protostars (Koyama et al. 1996) as well as of magnetically active, weak-lined TTS (Skinner et al. 1997). These flares are characterized by an order of magnitude or more increase in X-ray flux accompanied by a significant hardening of the X-ray spectrum, and have durations of order days. Nevertheless, flaring activity seems a more plausible explanation for the *ASCA* count rate increases observed for TW Hya than



does, e.g., rotational modulation of coronal features (§4.3).

## 4. Discussion

### 4.1. The Soft, “Quiescent” X-ray Spectrum of TW Hya

Comparison of the results of model fits to the *ROSAT* and *ASCA* spectra (Table 2) indicates that the characteristic emitting region temperatures and X-ray luminosity of TW Hya changed little between the epochs of the *ROSAT* and *ASCA* observations, although they were obtained about 5.5 years apart. These results indicate that the *ASCA* and *ROSAT* spectra are generally characteristic of a “quiescent” state of TW Hya, although we apparently detected relatively modest, short-lived flares during the *ASCA* observation. Evidently, the quiescent X-ray spectrum of TW Hya ( $kT \sim 0.85$  keV for the “hard” component) is much softer than the quiescent X-ray spectra of embedded protostars ( $kT \sim 6$  keV; Koyama et al. 1996) or of relatively young TTS ( $kT \sim 3$  keV for the hard components; Skinner et al. 1997, Skinner & Walter 1998). Given KZWF’s conclusion that TW Hya is unusually “old” for a classical TTS, this comparison suggests a trend toward softer X-ray emission as a TTS settles onto the main sequence (see also Skinner & Walter 1998). This trend is evidently accompanied by only a modest decrease, if any, in X-ray luminosity; indeed, the ratio of X-ray to bolometric luminosity increases throughout a late-type star’s pre-main sequence evolution (KZWF). Further X-ray observations may establish whether or not TW Hya exhibits powerful X-ray flares such as have been observed for many other TTS, whether its apparent short-term variability is periodic, and whether its “quiescent” X-ray spectral distribution varies with time.

### 4.2. X-ray Ionization of the TW Hya Molecular Disk

The *ASCA* data likely well characterize the X-ray spectrum that is incident on surface or subsurface layers of the circumstellar molecular disk surrounding TW Hya. As described by Glassgold et al. (1997), X-ray radiation incident on a circumstellar molecular disk can partially ionize the disk if the incident radiation is sufficiently intense and hard. The position-dependent ionization rate and resulting electron fractions, though small, may be sufficient to produce stratified disk instabilities that can govern accretion onto the star as well as protoplanetary accretion at the disk midplane (Glassgold et al.). Also, X-ray ionization of molecular gas may play a central role in determining circumstellar chemistry and, in particular, may explain the enhanced abundance of  $\text{HCO}^+$  measured at TW

Hya (KZWF). Thus, the X-ray emission from TW Hya could be an important factor in determining the chemical composition of protoplanetary gas and may play a central role in the formation of any protoplanets themselves, provided there is sufficient X-ray flux to effectively ionize molecular material in the disk.

The Glassgold et al. (1997) and Igea & Glassgold (1999) models are formulated for hypothetical star-disk systems. It is worthwhile, therefore, to consider how closely these models actually resemble the TW Hya system, which represents in many respects the prototypical example of an X-ray-bright TTS surrounded by a circumstellar, molecular disk. We have demonstrated above that TW Hya displays a relatively soft X-ray spectrum; of the spectra considered in the Glassgold et al. (1997) models, for example, the TW Hya spectrum evidently more closely resembles their assumed “soft” (1 keV) spectrum than their “hard” (5 keV) spectrum. As Glassgold et al. point out, the greater penetration of hard X-rays enhances the ionization rates of the hard model relative to the soft model, for a given X-ray luminosity  $L_x$ . Hence, the ionization rates produced by the X-ray field of TW Hya fall short of those that would be produced by, e.g., a younger T Tauri star or protostar of comparable  $L_x$  (but harder X-ray spectrum) that is surrounded by a molecular disk of comparable mass. However, the X-ray luminosity of TW Hya is an order of magnitude larger than that assumed for the central star in the Glassgold et al. models. Therefore, as the X-ray ionization rate at a given point in the disk is proportional to  $L_x$ , the ionization structure of the TW Hya disk may more closely resemble that of the Glassgold et al. 5 keV model than their 1 keV model (see Fig. 2 of Glassgold et al.). Moreover, the *ASCA* data demonstrate that, despite its relatively soft spectrum,  $\sim 10\%$  of the X-ray luminosity of TW Hya, or  $2 \times 10^{-29}$  ergs  $s^{-1}$ , emerges at energies  $> 2$  keV. Hence there is clearly ample hard X-ray flux to produce significant X-ray ionization of the TW Hya molecular disk, according to the Glassgold et al. and Igea & Glassgold models.

The foregoing comparison suggests that a more detailed analysis, along the lines of that carried out by Igea & Glassgold (1999) but tailored to conditions appropriate for TW Hya, would be of great interest. Such an analysis should take into account the fact that the X-ray spectrum of TW Hya evidently is dominated by emission lines at energies near 1 keV (§3.2.1), and that its molecular disk mass ( $\sim 7 \times 10^{28}$  g, or  $\sim 12$  Earth masses; KZWF) is a factor  $\sim 100$  smaller than that of the “canonical” minimum mass solar nebula. The latter constraint implies large ionization rates near the TW Hya disk mid-plane, relative to the ionization rates characteristic of models tailored to the minimum mass solar nebula.

### 4.3. $N_H$ : Constraints on Circumstellar and Viewing Geometries

The range in absorbing column indicated by the fits to the PSPC and SIS spectra constrains both the distribution of circumstellar material and our view of the star through this material. Assuming that  $N_H$  is dominated by circumstellar (as opposed to interstellar) extinction at the large neutral H densities implied by the detection of HCN line emission ( $n_{H_2} > 10^7 \text{ cm}^{-3}$ ; KZWF), the value of  $N_H$  derived from the SIS data ( $N_H \sim 2.9 \times 10^{21} \text{ cm}^{-2}$ ) suggests the column length along the line of sight to the star is  $l < 3 \times 10^{14} \text{ cm}$  ( $l < 20 \text{ AU}$ ). The PSPC result for  $N_H$  would impose a more stringent upper limit of  $l < 5 \times 10^{13} \text{ cm}$  ( $l < 3 \text{ AU}$ ). Based on CO line strengths and ratios, KZWF concluded that the projected radius of the molecular line emitting region is  $\sim 60 \text{ AU}$ . Thus, if the material responsible for the absorption measured in the X-ray spectra of TW Hya resides in the same circumstellar structure as is responsible for the molecular line emission, then this structure is flattened and is viewed from high latitude (if viewed edge-on, the TW Hya disk would have a molecular column density  $N_{H_2} > 10^{22} \text{ cm}^{-2}$ ). On the other hand, the presence of a considerable column depth of ionized gas is reflected in the fact that TW Hya displays a huge H $\alpha$  equivalent width (e.g., KZWF). Such a large H $\alpha$  EW likely results from a large mass loss rate (e.g., Bouvier et al. 1995) and this material most likely is ejected along the poles of the star. Hence the X-ray absorption may be produced in an extended, ionized stellar wind. In either case, the results for  $N_H$  appear to support the conclusion that the dense, relatively cold ( $T \sim 100 \text{ K}$ ) region of circumstellar molecular gas and dust detected in the millimeter and submillimeter wavelength regime resides in a flattened structure surrounding TW Hya that is viewed nearly pole-on (Zuckerman et al. 1995; KZWF).

### 4.4. Variability of Optical Photometry and X-rays

Photometry published in Rucinski & Krautter (1983) indicated that TW Hya displays large-amplitude ( $\sim 0.5 \text{ mag}$ ) variability over short (1-day) timescales. Herbst & Koret (1988) derived periods of 1.28 days and 1.83 days from their own *UBV* photometric monitoring and from the older dataset of Rucinski & Krautter, respectively. Herbst & Koret attributed the variability to rotational modulation of a hot spot. More recently, Mekkadén (1998) derived a period of 2.196 days from independent photometric monitoring and claimed that this longer period satisfies all available photometry, including the monitoring data analyzed by Herbst & Koret. However, the phases of maximum and minimum light can be seen to shift randomly in the folded light curves for various observing epochs presented by Mekkadén.

Given the apparent inconsistency in the various published results for the period of TW

Hya, we examined archival optical ( $V$  band) photometry of TW Hya obtained during the course of the Hipparcos astrometry mission. This photometry is rather sparsely sampled, but extends over a long temporal baseline encompassing the time period of the various photometric datasets presented by Mekkaden (1998). In addition to revealing  $V$  fluctuations of  $\sim 0.2$  mag over the course of a day or so, the Hipparcos data well illustrate the larger, longer-term optical variability of TW Hya (Fig. 2a). Indeed, these data include the brightest and faintest  $V$  magnitudes (minimum  $V = 10.58 \pm 0.03$ ; maximum  $V = 11.38 \pm 0.04$ ), and hence display the largest amplitude of  $V$  band variation ( $\Delta V = 0.8$  mag), observed thus far for TW Hya.

We have folded the Hipparcos  $V$  photometry according to the various periods cited in the literature (Fig. 2b-d). There is considerable scatter in each of these folded lightcurves, and no regular variation can be discerned. We conclude that none of the published periods well describes the Hipparcos photometry. The Hipparcos data therefore cast doubt on the existence of well-defined, short-period optical variability of TW Hya, such as would be due to rotational modulation.

A general problem with the interpretation of the optical variability in terms of rotational modulation is the likely viewing geometry. Both Herbst & Koret (1988) and Mekkaden (1998) contend that the wavelength dependence of the variability amplitude of TW Hya is best interpreted as rotation of a hot (as opposed to cool) spot and, hence, may indicate the presence of an accretion hotspot at the boundary layer between star and disk. There now exists independent evidence for the presence of a circumstellar disk (Weintraub et al. 1989; KZWF). However, there is accumulating evidence that the disk is viewed nearly pole-on (§4.3; KZWF), and the measured  $v \sin i < 15 \text{ km s}^{-1}$  (Franchini et al. 1992; Webb 1998, private comm.) suggests the star itself is also viewed from a high latitude. Even if the system is viewed nearly, but not precisely, pole-on, a model that interprets the variation of  $UBV$  radiation in terms of the rotation of an accretion hotspot requires either that the hotspot is very near the star’s equator or that the star’s rotation axis is not well aligned with the disk axis. Neither idea is favored by contemporary protostellar accretion theory (e.g., Shu et al. 1997).

Accepting for the moment that Herbst & Koret (1988) and Mekkaden (1998) have detected rotational modulation in the light curve of TW Hya, any of the periods derived by these investigations would make TW Hya one of the fastest rotating classical TTS known. Generally, however, its somewhat erratic photometric behavior resembles that of other classical TTS stars, many of which exhibit temporal variations in and disappearances/reappearances of photometric periodicity (Bouvier et al. 1995). Like Herbst & Koret and Mekkaden, Bouvier et al. interpret the variability of the stars in their

classical TTS sample in terms of rotational modulation of hot spots. However, the changes, disappearances, and reappearances of periodicity in the photometry of TW Hya and other classical TTS suggest that quasi-random flaring, perhaps caused by short-lived, small-scale accretion events, might better explain their short timescale optical variability. Similar processes may be responsible for the X-ray outbursts seen by *ASCA* (Fig. 2).

The longer-term optical variability of TW Hya, on the other hand, may be related to changes in X-ray absorbing column (§3.2.1). The fits to the PSPC and SIS spectra indicate that  $N_H$ , and hence  $A_V$ , may have changed by a factor  $\sim 6$  over the intervening  $\sim 5.5$  yr. Based on conversion factors from  $A_V$  to  $N_H$  listed in Ryter (1996) and Neuhauser, Sterzik, & Schmitt (1995), the results for  $N_H$  correspond to  $A_V \sim 0.25$  and  $A_V \sim 1.5$  for the epochs of the *ROSAT* and *ASCA* data, respectively. Given the star’s UV and near-IR excesses, it is difficult to determine reddening via e.g. observed vs. intrinsic  $B - V$  color (Rucinski & Krautter 1983); hence these results for  $A_V$  serve as perhaps the most reliable indications yet obtained of the magnitude and variability of visual extinction toward TW Hya.

The large range inferred for  $A_V$  raises the possibility that the long timescale, large amplitude optical variability of TW Hya is due to variable circumstellar obscuration. In this regard it is intriguing that the Hipparcos data appear to show long-term ( $\sim 600$  day) periodicity characterized by steep declines in  $V$  followed by more gradual recoveries. This variation is reminiscent of, though not nearly as dramatic as, the behavior of R CrB stars, which vary by many magnitudes in the optical due to the formation and then gradual dispersal of dust clouds along the line of sight to the stars (Clayton 1996). Observations that the amplitude of variation increases steeply with decreasing wavelength and that the degree of optical polarization changes with time (Mekkaden 1998) are consistent with variable obscuration of the star by dust. Furthermore the difference in inferred  $A_V$  between the epochs of the *ROSAT* and *ASCA* observations (1.2 mag) is on the order of the amplitude of  $V$  band variation measured by Hipparcos (0.8 mag). On this basis, we would predict that TW Hya was at or near its faintest at the time of the *ASCA* observations (June 1997; J.D. 2450626), as the  $A_V$  inferred from the *ASCA* data is large. Unfortunately we are not aware of the existence of optical photometry that might provide a test of this prediction. However, at the approximate time of the *ROSAT* pointed observations (Dec. 1991; J.D. 2448602), for which we infer a relatively small  $A_V$  and therefore we anticipate that TW Hya was quite bright optically, Hipparcos measured only  $V \sim 11.0$  (Fig. 2a) — roughly the median of the Hipparcos  $V$  band measurements. Thus, while the large range of  $A_V$  inferred from the X-ray data is suggestive of the presence of variable obscuration, it is not clear that these values provide an accurate measure of the relative  $V$  magnitude of TW Hya.

In contrast to the episodic dust formation and dispersal characteristic of R CrB stars,

we speculate that the appearance and gradual disappearance of dust clouds along the line of sight to TW Hya might be produced by episodes in which infalling disk material is partially accreted and partially redirected into polar jets or outflows. This explanation seems consistent with the variability of optical continuum and H $\alpha$  emission from TW Hya (Mekkaden 1998) as well as its X-ray variability. Further contemporaneous X-ray spectroscopy and optical photometric and polarimetric monitoring would test the hypothesis that the long-term variability of TW Hya and other classical T Tauri stars is due to variable circumstellar extinction.

## 5. Conclusions

We have obtained and analyzed *ASCA* data and re-analyzed archival *ROSAT* data for the nearby, isolated classical T Tauri star TW Hya. We find that both *ROSAT* and *ASCA* spectra are well fit by a two-component Raymond-Smith thermal plasma model, with characteristic temperatures of  $T \sim 1.7$  MK and  $T \sim 9.7$  MK and X-ray luminosity of  $L_x \sim 2 \times 10^{30}$  ergs s $^{-1}$ . Prominent line emission, likely arising from highly ionized species of Fe, is apparent in the *ASCA* spectra at energies  $\sim 1$  keV, while the GIS spectrum displays a weak hard X-ray excess at energies  $> 2$  keV. Although modest flaring is apparent in the *ASCA* light curve, the overall similarity of the X-ray spectra inferred from the *ASCA* and *ROSAT* observations suggests that the X-ray data obtained to date are characteristic of a “quiescent” TW Hya.

There is evidence that the absorption of the X-ray spectrum of TW Hya may have changed in the  $\sim 5.5$  year interval between *ROSAT* and *ASCA* observations. The apparent long-term change in  $N_H$  and the appearance of short-lived flares in the *ASCA* data appear to be related to the large amplitude optical variability of TW Hya on both long and short timescales; neither the X-ray nor optical variability appears to be well explained by rotational modulation.

Since TW Hya appears to be a single star of age  $\sim 10$  Myr that is surrounded by a circumstellar molecular disk (KZWF), the *ASCA* spectra offer an indication of the X-ray spectrum of the young Sun during the epoch of Jovian planet building. These spectra indicate that the hard X-ray flux from TW Hya ( $\sim 2 \times 10^{29}$  ergs s $^{-1}$  at energies  $> 2$  keV) is sufficient to produce substantial ionization of its circumstellar molecular disk.

Further X-ray spectroscopic and monitoring observations of TW Hya might find the star in a strong, longer-lived flaring state, and would better establish whether or not the physical conditions responsible for its “quiescent” spectrum are stable. In this regard, we

note that TW Hya will be observed by both the Chandra X-ray Observatory (CXO) and the X-ray Multimirror Mission (XMM) during their first years of operation<sup>2</sup>. Chandra and XMM observations of TW Hya should far surpass the *ASCA* and *ROSAT* results presented here in terms of spectrum quality, and thus should provide additional insight into the nature of the X-ray emission from this seminal young, Sun-like star. In particular, high-resolution (gratings spectrometer) CXO and XMM spectra of TW Hya will provide critical tests of our conclusions that the X-ray spectrum of TW Hya is coronal in origin and that the features seen near 1 keV in *ASCA* and *ROSAT* spectra are formed by a blended complex of highly ionized iron lines. Low-resolution (CCD) spectra resulting from both missions will provide additional measures of the degree and variability of intervening circumstellar absorption.

Primary support for this work was provided by NASA *ASCA* data analysis grant NAG5–4959 to M.I.T. Research by J.H.K., D.P.H., and N.S.S. at M.I.T. is also supported by the Chandra X-ray Observatory Science Center as part of Smithsonian Astrophysical Observatory contract SVI–61010 under NASA Marshall Space Flight Center. Support for research by D.A.W. and J.H.K. was also provided by NASA Origins of Solar Systems program grant NAG5–8295 to Vanderbilt University.

## REFERENCES

- Bouvier, J., Covino, E., Kovo, O., Martin, E.L., Matthews, J.M., Terranegra, L., & Beck, S.C. 1995, *A&A*, 299, 89
- Carkner, L., Feigelson, E.D., Koyama, K., Montmerle, T., & Reid, I.N. 1996, *ApJ*, 464, 286
- Clayton, G.C. 1996, *PASP*, 108, 225
- Feigelson, E.D. 1996, *ApJ*, 468, 306
- Franchini, M., Covino, E., Stalio, R., Terranegra, L., & Chavarria-K., C. 1992, *A&A*, 256, 525
- Glassgold, A.E., Najita, J., & Igea, J. 1997, *ApJ*, 480, 344
- Herbst, W., & Koret, D.L.. 1988, *AJ*, 96, 1949

---

<sup>2</sup>As of this writing, CXO was scheduled for launch in summer 1999, while XMM launch was scheduled for January 2000.

- Hoff, W., Henning, Th., & Pfau, W. 1998, *A&A*, 336, 242
- Igea, J., & Glassgold, A.E. 1999, *ApJ*, in press
- Kastner, J.H., Zuckerman, B., Weintraub, D.A., & Forveille, T. 1997, *Science*, 277, 67  
(KZWF)
- Koyama, K., Hamaguchi, K., Ueno, S., Kobayashi, N., & Feigelson, E.D. 1996, *PASJ*, 48,  
L87
- Mekkaden, M.V. 1998, *A&A*, 340, 135
- Montmerle, T., Feigelson, E.D., Bouvier, J., & André, P. 1993, in *Protostars and Planets  
III*, eds. E.H. Levy & J.I. Lunine (Tucson: U. Arizona Press), p. 689.
- Neuhauser R., Sterzik, M.F., & Schmitt J. H. M. M. 1995, *A&A*, 233, 178
- Omodaka, T., Kitamura, Y., & Kawazoe, E. 1992, *ApJ*, 396, L87
- Raymond, J. C., & Smith, B. W. 1976, *ApJS*, 35, 419
- Rucinski, S.M., & Krautter, J. 1983, *A&A*, 121, 217
- Ryter, C.E. 1996, *Ap&SS* 236, 285
- Shu, F.H., Shang, H., Glassgold, A.E., & Lee, T. 1997, *Science*, 277, 1475
- Skinner, S.L., Gudel, M., Koyama, K., & Yamauchi, S. 1997, *ApJ*, 486, 886
- Skinner, S.L., & Walter, F. M. 1998, *ApJ*, 509, 761
- Soderblom, D.R., et al. 1998, *ApJ*, 498, 385
- Voges, W., et al. 1998, in *New Horizons from Multi-Wavelength Sky Surveys*, Proc. of IAU  
Symp. 179, eds. B. J. McLean, D. A. Golombek, J. J. E. Hayes, & H. E. Payne  
(Kluwer Academic), p. 33.
- Webb, R.A., Zuckerman, B., Platais, I., Patience, J., White, R.J., Schwartz, M.J.,  
McCarthy, C. 1999, *ApJ*, 512, L63
- Weintraub, D.A., Sandell, G., & Duncan 1989, *ApJ*, 340, L69
- Weintraub, D.A., Saumon, D., Kastner, J.H., & Forveille, T. 1999, *ApJ*, submitted
- Wichmann, R., Bastian, U., Krautter, J., Jankovics, I., & Rucinski, S.M. 1998, *MNRAS*,  
301, L39



Zuckerman, B., Forveille, T., & Kastner, J.H. 1995, *Nature*, 373, 494

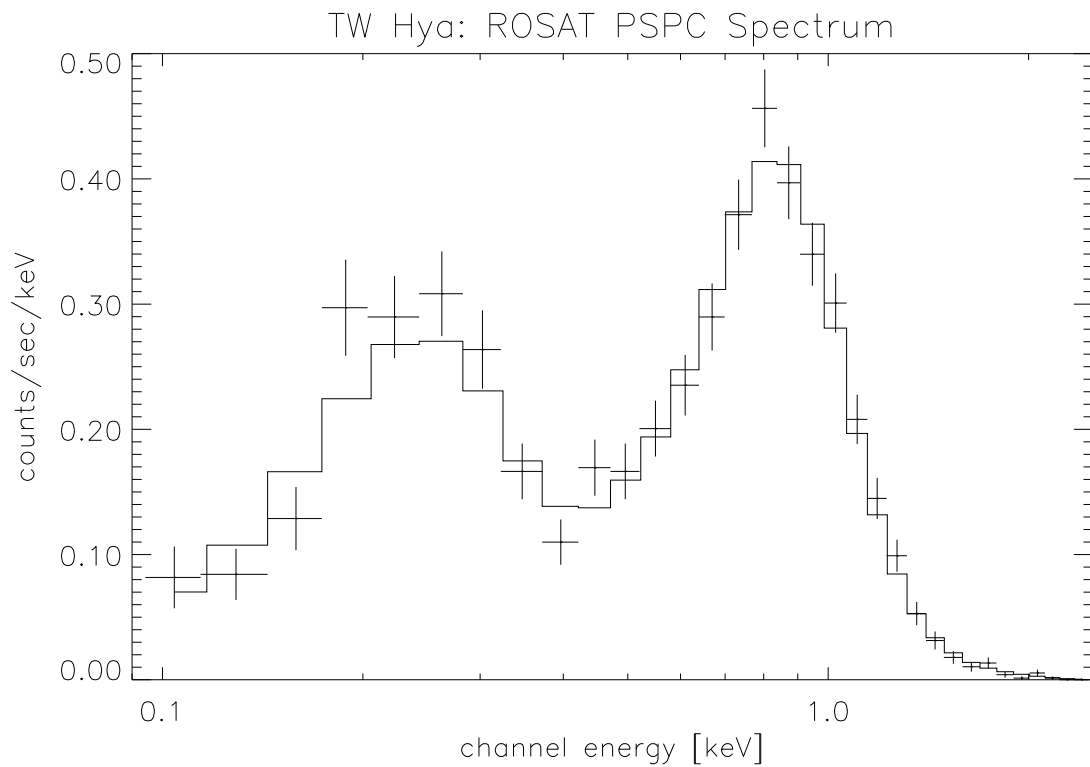


Fig. 1.— *ROSAT* PSPC spectrum measured toward TW Hya (crosses), with the best-fit Raymond-Smith plasma model overlaid (histogram). The depression in both data and model near 0.4 keV is a result of absorption by the *ROSAT* mirror.

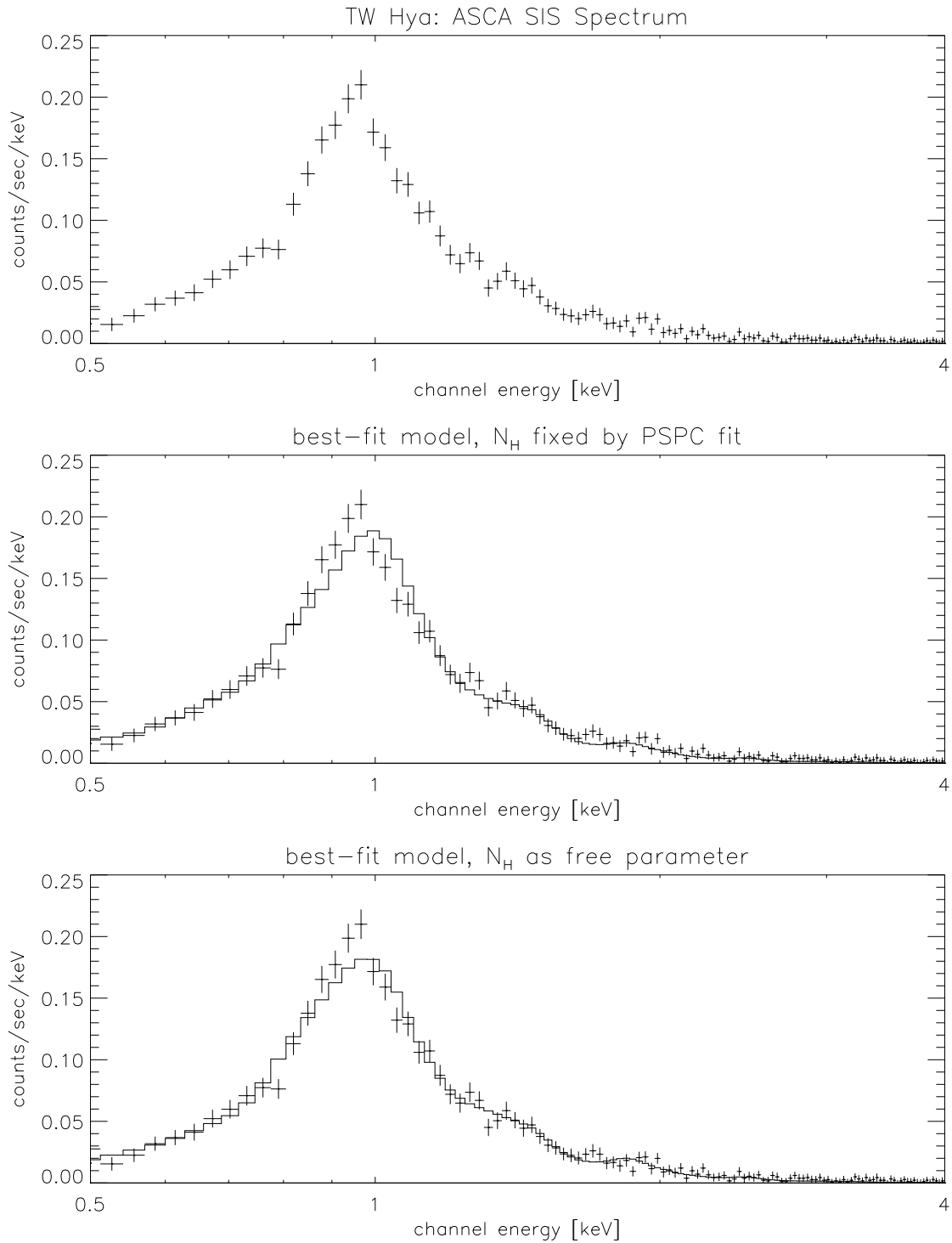


Fig. 2.— Background-subtracted *ASCA* SIS0 + SIS1 spectrum (top panel). The lower two panels show these data (crosses) overlaid with best-fit two-component Raymond-Smith thermal plasma models (histograms), with absorbing column fixed by the results of PSPC fitting (middle panel) and with absorbing column as a free parameter (bottom panel).

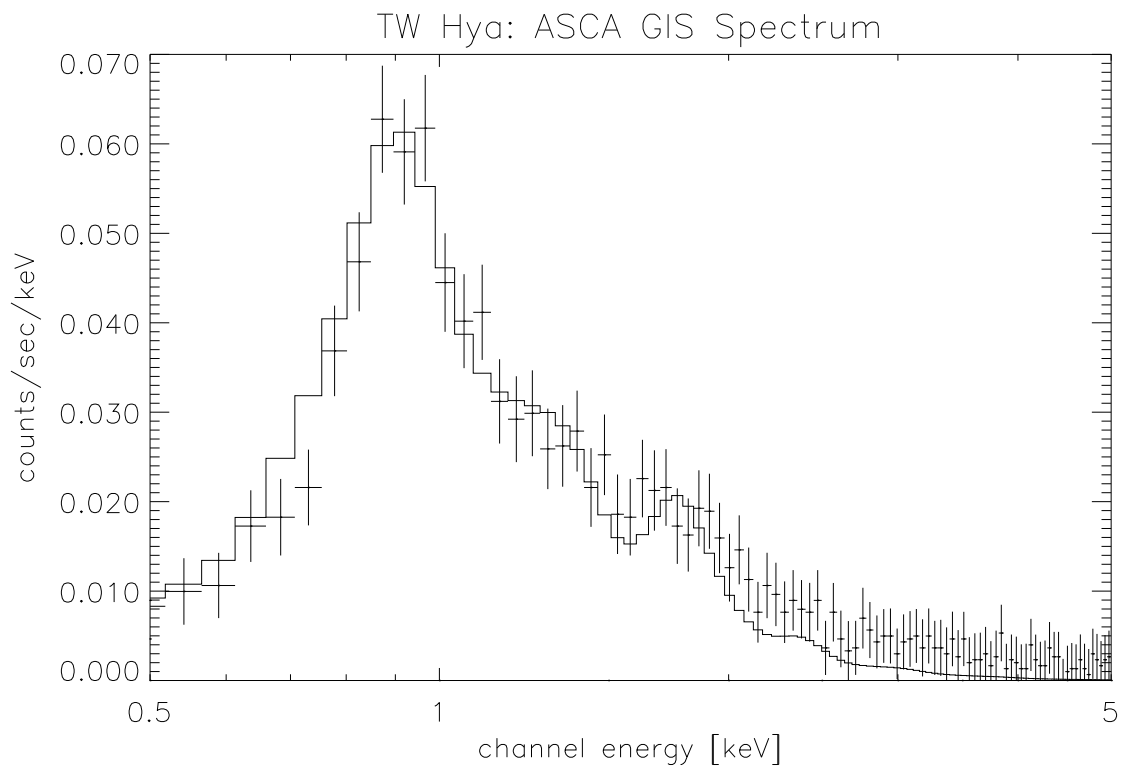


Fig. 3.— Background-subtracted *ASCA* GIS2 + GIS3 spectrum (crosses), with Raymond-Smith thermal plasma model (histogram) overlaid. The characteristic temperatures and  $N_H$  of this model are identical to the model overlaying the SIS data in the bottom panel of Fig. 2.

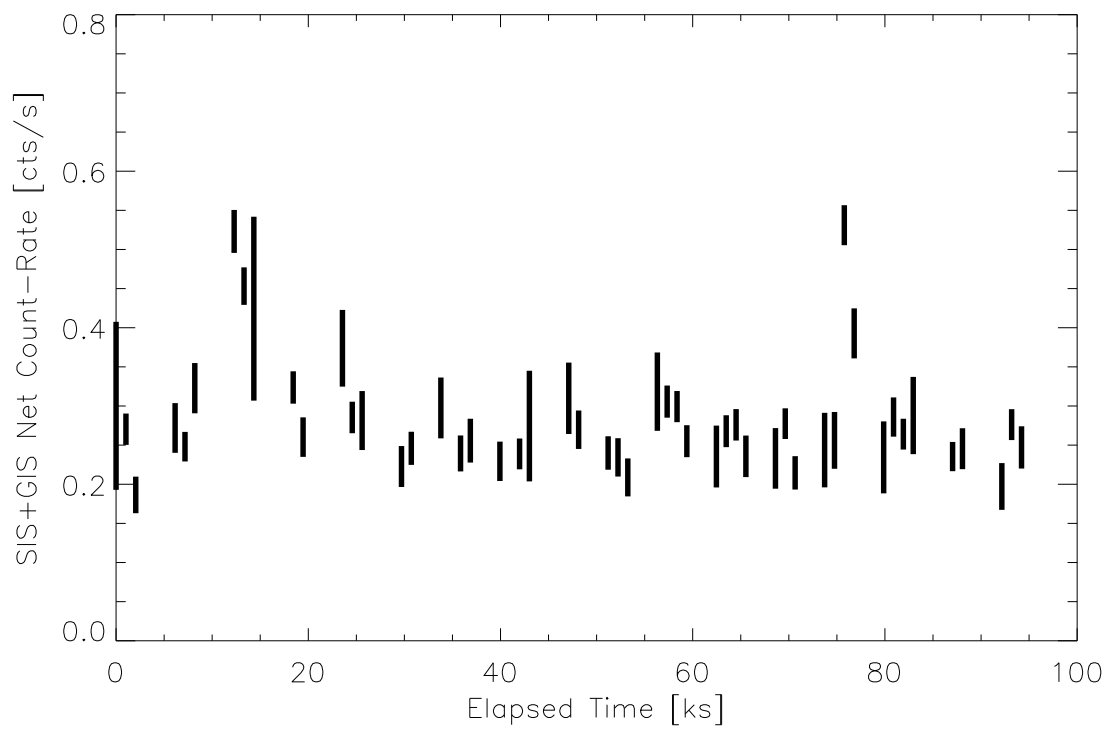


Fig. 4.— Combined SIS and GIS light curve of TW Hya. The width of the time bins is 1024 s. Symbols show  $\pm 1\sigma$  error bars and are centered on the measured count rate. Note the short-lived ( $\sim 2$  ksec duration) “flares” at elapsed times of  $\sim 12$  and  $\sim 76$  ksec.

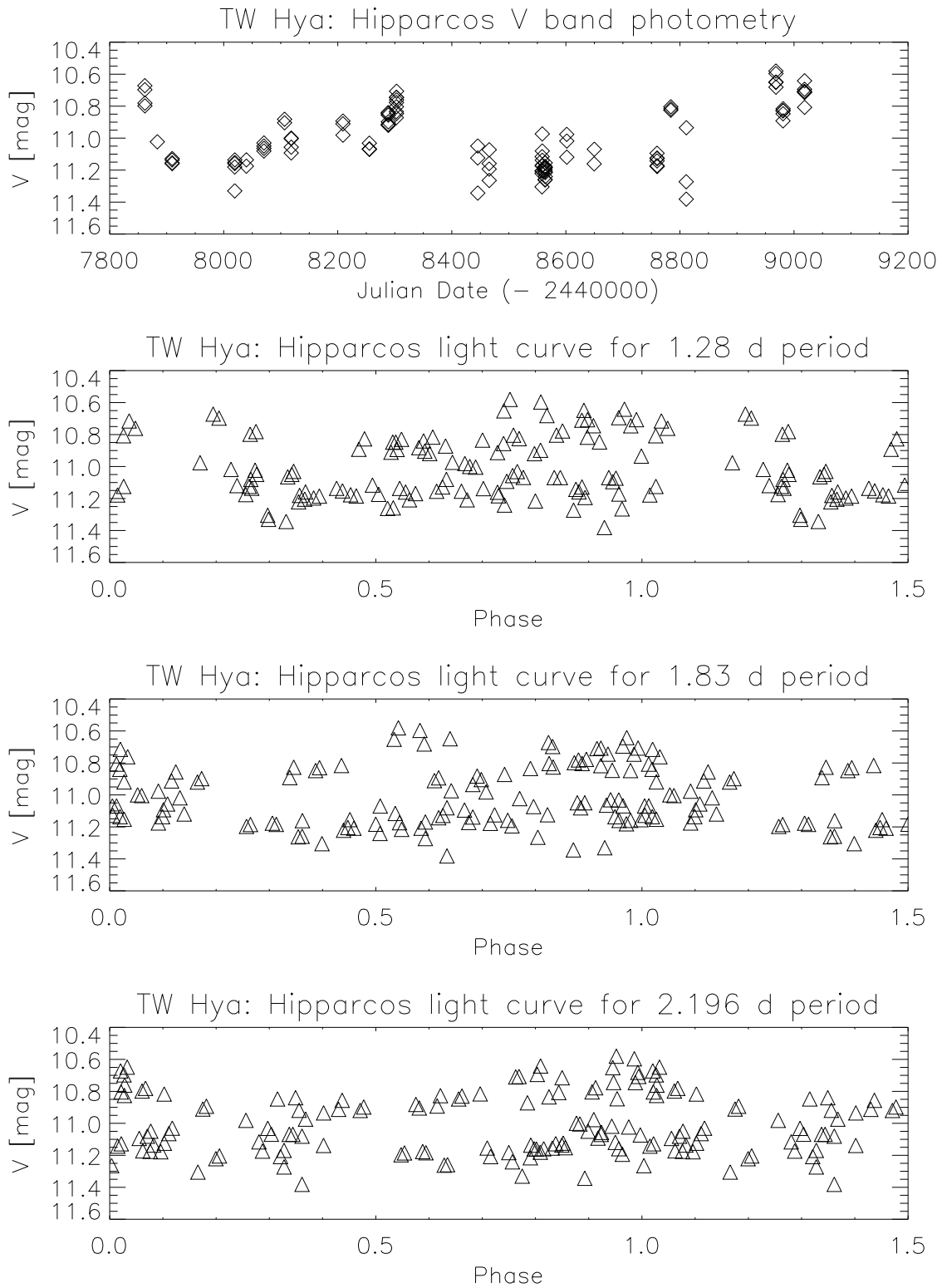


Fig. 5.— Hipparcos V band light curve of TW Hya (top). The remaining 3 panels show phase diagrams constructed by folding the Hipparcos V band photometry according to various periods derived in the literature (see §4.4).

TABLE 1  
*ASCA* COUNTS AND COUNT RATES FOR TW HYA

Detector	Total Counts		Count Rate (ks <sup>-1</sup> )	
	Source	Background	Source	Background
SIS0	4499	570	145±2	18±1
SIS1	3368	662	112±2	22±1
GIS2	2027	366	65±1	12±1
GIS3	2273	148	72±1	4.7±0.4

TABLE 2  
 TW HYA: X-RAY SPECTRAL FIT RESULTS

Data	$kT_1$ (keV)	EM <sub>1</sub> <sup>a</sup> (10 <sup>52</sup> cm <sup>-3</sup> )	$kT_2$ (keV)	EM <sub>2</sub> <sup>a</sup> (10 <sup>52</sup> cm <sup>-3</sup> )	$N_H$ (10 <sup>20</sup> cm <sup>-2</sup> )	$\chi^2$ (DOF) <sup>b</sup>	$F_X$ <sup>c</sup> (10 <sup>-12</sup> ergs cm <sup>-2</sup> s <sup>-1</sup> )	$F_{X,0}$ <sup>c</sup> (10 <sup>-12</sup> ergs cm <sup>-2</sup> s <sup>-1</sup> )
ROSAT PSPC	0.14±0.02	5.9±0.4	0.85±0.09	2.7±0.4	5.2±3.7	0.88 (25)	2.9	6.0
ASCA SIS	0.22±0.02	1.2±0.4	0.98±0.02	3.9±0.2	5.0 <sup>d</sup>	0.90 (130)	2.2	2.5
ASCA SIS	0.15±0.02	17±12	0.86±0.02	5.5±0.7	29±4	0.76 (129)	2.2	4.2
ASCA GIS	...	...	0.98 <sup>d</sup>	5.5±0.4	5.0 <sup>d</sup>	0.47 (189)	2.4	2.8
ASCA GIS	...	...	0.86 <sup>d</sup>	7.0±0.5	29 <sup>d</sup>	0.50 (189)	2.4	4.6

<sup>a</sup>Emission measure, assuming the distance  $D = 57$  pc.

<sup>b</sup>Degrees of freedom.

<sup>c</sup>Absorbed X-ray flux ( $F_X$ ) and intrinsic X-ray flux ( $F_{X,0}$ ) in 0.1 to 2.4 keV band for ROSAT PSPC spectrum and in the 0.5 to 10.0 keV band for ASCA spectra.

<sup>d</sup>Parameter fixed during spectral fitting.